LYSTROSAURUS MURRAYI (THERAPSIDA, DICYNODONTIA): BONE HISTOLOGY, GROWTH AND LIFESTYLE ADAPTATIONS

by SANGHAMITRA RAY*, ANUSUYA CHINSAMY† *and*
SASWATI BANDYOPADHYAY‡

*Geological Studies Unit, Indian Statistical Institute, 203 B. T. Road, Kolkata 700108, India; current address: Department of Geology and Geophysics, Indian Institute of Technology, Kharagpur 721302, India; e-mail: sray@gg.iitkgp.ernet.in
†Department of Zoology, University of Cape Town, Rondebosch 7701, Cape Town, South Africa; e-mail: achinsam@botzoo.uct.ac.za
‡Geological Studies Unit, Indian Statistical Institute, 203 B. T. Road, Kolkata 700108, India; e-mail: saswati@isical.ac.in

Abstract: Examination of the bone microstructure of *Lystrosaurus murrayi* from India and South Africa reveals a predominance of fibrolamellar bone tissue, which suggests rapid periosteal osteogenesis and an overall fast growth. Four distinct ontogenetic stages have been identified based on tissue type, organization of the primary osteons, incidence of growth rings, secondary reconstruction and endosteal bone deposition. An indeterminate growth strategy is proposed for *Lystrosaurus*. Inter-elemental histovariability suggests differential growth rate of the skeletal elements within the same individual, and among different individuals. The high cortical thickness of the dorsal ribs, an extensive secondary reconstruction in the cortical region of different skeletal elements that resulted in erosionally enlarged channels from the perimedullary to the midcortical region, and trabecular infilling of the medullary region even in the diaphyseal sections of the limb bones suggest at least a semi-aquatic lifestyle for *L. murrayi*.

Key words: dicynodont, fibrolamellar, growth, histology, lifestyle.

THE dicynodont *Lystrosaurus*, which appeared in the Late Permian and crossed the Permo-Triassic boundary (King and Jenkins 1997; Smith and Ward 2001), is common in the Early Triassic sediments of the Beaufort Group, Karoo Supergroup, South Africa. Originally described as *Dicynodon murrayi* (Huxley 1859) and *Ptychognathus* (Owen 1860), it was renamed as *Lystrosaurus* by Cope (1870). Its cranial morphology is distinctive and includes a strongly down-turned snout, extensive premaxilla, nostrils situated high up on the snout and a short temporal area (Broom 1932; Cluver 1971; King and Cluver 1991). Currently, several species of *Lystrosaurus* are recognized from South Africa based on such characters as the extent of snout development and the presence of a nasofrontal ridge and a prefrontal boss. Other than South Africa, the species *L. murrayi*, *L. platyceps* and *L. maccaigi* are known from Antarctica and India (Tripathi and Satsangi 1963; Colbert 1974; Cosgriff *et al.* 1982) whereas several other endemic species have been reported from Russia, China and India (King 1991). Early studies by Watson (1912, 1913), Broom (1932) and Cluver (1971) suggested that *Lystrosaurus* was essentially an aquatic animal that inhabited a swampy environment.

However, King (1991) concluded that the skeletal characteristics of *Lystrosaurus* such as the flaring/wide scapular blade, lateromedially extended and flattened antebrachium, and short and robust manus are also present in digging animals, and did not support the hypothesis that it was aquatic. The down-turned snout, large premaxilla and short temporal area of *Lystrosaurus* resulted in a powerful bite, which was necessary for chopping and shredding plant matter (King and Cluver 1991). Recently, small articulated skeletons of *Lystrosaurus* were found in burrow casts assigned to the ichnogenus *Histioderma* (Groenwald 1991; Retallack *et al.* 2003). However, Retallack *et al.* (2003) suggested that *Lystrosaurus* species were amphibious/semi-aquatic in nature, waded into water for food and probably lived in a wide range of habitats as they occur in almost all types of Triassic palaeosols/pedotypes including those that supported submerged vegetation. Hence, the peculiar cranial features and varied interpretations of lifestyle (Watson 1912; Cluver 1971; King 1991; King and Cluver 1991; Retallack *et al.* 2003) make *Lystrosaurus* an enigmatic dicynodont.

Bone histology provides valuable information on aspects of an animal's life such as growth strategy,

biomechanics and lifestyle, as histological and morphological integrity are generally maintained even after fossilization. Previous work on dicynodont bone microstructure has contributed significantly to understanding various aspects of their biology (e.g. Ricqlès 1972, 1976; Chinsamy and Rubidge 1993; Ray and Chinsamy 2004). Based on bone histology this paper provides an assessment of the palaeobiology of the type species of *Lystrosaurus*, *L. murrayi*. The aims of the study are to elucidate growth pattern, document histovariability and evaluate the mode of life of *Lystrosaurus*.

Institutional abbreviations. ISIR, Indian Statistical Institute, Kolkata, India; SAM-PK-K, South African Museum, Cape Town, South Africa.

MATERIAL AND METHODS

A series of skeletal elements (humeri, femora, radii, ulnae, tibiae, fibulae, ribs, scapulae, clavicles, centrum and distal phalanx) of positively identified *L. murrayi* were examined. These elements were taken from 11 partial and complete skeletons collected from various localities of the Early Triassic *Lystrosaurus* Assemblage Zone, Beaufort Group, South Africa (Table 1). The specimens bearing the same registration number but differentiated by 'a' or 'b' indicate the association of two individuals. We also examined several disarticulated skeletal elements (humeri, femora, tibia, fibula, clavicle and dorsal rib fragments) of *L. murrayi*, collected from a monospecific bone bed of the Early Triassic Panchet Formation, Damodar Basin, India (Table 2).

The different parameters of undistorted limb bones of *L. murrayi* in the collection were measured using Mitutuyo digimatic calipers, which have a precision of

TABLE 2. *Lystrosaurus murrayi.* Localities and skeletal elements of the specimens examined for histology and recovered from the Early Triassic Panchet Formation, Damodar Basin, India. Asterisk (*) indicates measurement of diameter. All specimens from the Banspatali locality.

Specimen no.	Elements used for histology	Length (mm)
ISIR758	femur	36·77
ISIR756	femur	53·77
ISIR765	femur	57·23
ISIR762	humerus	60·87
ISIR757	femur	68·66
ISIR753	humerus	62·26
ISIR761	femur	75·69
ISIR763	humerus	70·73
ISIR751	humerus	72·84
ISIR750	humerus	79·72
ISIR764	femur	90·3
ISIR759	tibia	88·4
ISIR760	fibula	85·39
ISIR754	clavicle	12*
ISIR752	dorsal rib	9*

0·01 mm. These measurements were used to calculate predictive regression equations of the proximal, midshaft and distal diameter of the limb bones (Table 3) as outlined in Ray and Chinsamy (2004). The high coefficient of determination (r^2) suggests that the regression equations explain most of the variations (80–98 per cent) in the data (Peters 1989; Seebacher 2001). The equations obtained were then used to infer the total length of the partial limb bones, and to deduce the relative sizes of different individuals examined for osteohistology. For overall comparison, especially between the elements of the same individual, size classes were deduced from one of the lar-

TABLE 1. *Lystrosaurus murrayi.* Localities and skeletal elements of the specimens examined for histology and recovered from the Early Triassic *Lystrosaurus* Assemblage Zone, Beaufort Group, South Africa.

Locality	Specimen no.	Elements examined for histology	Length of different limb bones examined (mm)				
			HL	UL	RL	FL	TiL/FiL
Middelburg	SAM-PK-K8	left humerus, dorsal rib fragments	99	–	–	–	–
Harrismith	SAM-PK-K1415	dorsal rib fragments	–	–	–	–	–
	SAM-PK-3531	humerus, clavicle, dorsal rib	25·85	–	–	–	–
Meadows	SAM-PK-8991a	humerus, radius, ulna, scapula, tibia	101·88	78·6	68·02	–	75·48
	SAM-PK-8991b	humerus, femur	65·96	69·32	–	–	–
	SAM-PK-8796a	scapula, femur, tibia, phalanx	–	–	–	–	83·88
	SAM-PK-8796b	femur	–	–	–	92·72	–
Bethulie	SAM-PK-K8038	humerus	176·57	–	–	–	–
	SAM-PK-K8013	humerus, radius, ulna, ribs	135·68	117·92	84	–	–
	SAM-PK-K8012	scapula, vertebra, rib	–	–	–	–	–
Colesburg	SAM-PK-11184	humerus, radius, ulna, femur, rib	89·46	67·49	54·6	115·05	–

TABLE 3. Predictive regression equations for determining the propodial lengths and midshaft diameters of *L. murrayi*.

Propodials	n	Allometric equations	r^2
HL–HPD	6	$y = 0.9165x - 0.1065$	0.97
HL–HMD	8	$y = 0.8153x - 0.2975$	0.8
RL–RPD	6	$y = 1.1235x - 0.6097$	0.94
RL–RMD	6	$y = 1.1261x - 0.9466$	0.95
UL–UPD	6	$y = 0.7808x + 0.0317$	0.94
FL–FPD	8	$y = 0.825x - 0.0445$	0.85
FL–FMD	8	$y = 1.0016x - 0.8098$	0.82
TiL–TiDD	8	$y = 1.08196x - 0.5388$	0.92
FiL–FiDD	5	$y = 1.0346x - 0.7755$	0.98
HL–FL	9	$y = 0.833x + 0.4149$	0.97

gest specimens of *L. murrayi* (SAM-PK-K8038) in the collection of the South African Museum, as suggested by Chinsamy (1993*a*), Curry (1999), Horner *et al.* (2000) and Ray and Chinsamy (2004). These size classes were expressed as a percentage of adult size and were based on the relative size, gross skeletal morphology, allometry and histological characteristics of the various skeletal elements.

All the specimens were photographed, and morphological variations and standard measurements were noted. Specimens were embedded under vacuum in a clear resin, sectioned in the required direction, ground and polished, and examined under ordinary and polarized light (Chinsamy and Raath 1992; Ray and Chinsamy 2004). For determining growth strategy, emphasis was placed on the study of the mid-diaphyseal regions of the long bones as these were least remodelled and resulted in the better preservation of the primary bone tissue (Enlow 1963; Chinsamy and Dodson 1995; Sander 2000).

Histological terminology and definitions followed Francillon-Vieillot *et al.* (1990) and Ricqlès *et al.* (1991) unless specifically mentioned otherwise. Because most of the thin sections show sharp delineation between the relatively compact cortex and the medullary spongiosa (Text-figs 1–5), the cortical or relative bone wall thickness (RBT) and cortical porosity were measured following Bühler (1986), Chinsamy (1993*a*), Botha and Chinsamy (2000) and Ray and Chinsamy (2004). RBT was calculated as the ratio of the bone wall thickness to the cross-sectional diameter of the bone and expressed as a percentage. It was measured on the diaphyseal sections at 2·5× magnification. The porosity of the cortical area representing maximum vascularity was quantified as a percentage of total cortical area (Chinsamy 1993*b*), and was calculated by the image analysis software Jandel Sigma Scan Pro, version 4.0. This procedure was carried out for every alternate field of view at a magnification of 10× and about 10–15 fields were examined per slide. However, in some specimens the medullary region is completely filled with bony trabeculae resulting in a gradational transition between the cortex and the medulla. In such cases, it was not possible to measure RBT and/or cortical porosity.

HISTOLOGICAL DESCRIPTION

General features. The transverse sections of all the elements show an outer compact cortex surrounding a large medullary region. The predominant extracellular matrix of the cortex is woven fibred bone (Enlow 1969; Ricqlès *et al.* 1991) with a haphazard spatial arrangement of the collagen fibres and globular osteocyte lacunae. The humerus, rib and clavicle of the smallest individual, SAM-PK-3531, contain longitudinally orientated vascular channels with little or almost no osteonal deposits within them.

The skeletal elements of all the larger specimens except ISIR758 (discussed later) show fibrolamellar bone in the cortex. Most of the primary osteons are longitudinally orientated with mainly circumferential anastomoses, although this may vary from one element to the next, or even locally within the same element. Although secondary reconstruction is absent in SAM-PK-3531, the diaphyseal sections of the limb bones of larger individuals reveal extensive secondary reconstruction from the perimedullary region to the mid-cortical region. This resulted in erosionally enlarged and concentrically arranged resorption cavities and a very narrow compact periosteal cortex. Profuse secondary osteons are often visible in the deeper cortical region. The margin between the cortex and the medullary region, though distinct, is irregular. The medullary region is often completely filled with bony trabeculae of the cancellous bone.

Humerus. Numerous sections in the diaphyseal and metaphyseal regions of 12 humeri ranging in length (HL) from 25·85 to 176·57 mm were examined (Table 4). The smallest humerus (SAM-PK-3531: HL 25·85 mm, 14·64 per cent adult size) is characterized by a large medullary region surrounded by a narrow cortex (RBT 12·24 per cent; Table 5), an irregular periosteal margin (Text-fig. 1A), absence of growth rings and few radially orientated canals.

Diaphyseal sections of the humeri longer than that of SAM-PK-3531 (and presumably older) reveal that the cortex is predominantly composed of the fibrolamellar bone (Text-fig. 1B–C, Table 4). In humeri ranging between 70 and 100 mm in length the cortical thickness varies between 22·7 and 31·12 per cent (Table 5). The primary osteons are arranged in a laminar pattern, though this may vary from one humerus to the next, or even locally within the same humerus. For example, in SAM-PK-11184 reticular arrangement of the primary osteons is evident in the outer cortex whereas a laminar-subplexiform pattern is prevalent in the deeper cortex (Text-fig. 1B). Radially orientated channels, running from the midcortex to the outer cortex, are usually present in the region of the deltopectoral crest (such as SAM-PK-K8). In SAM-PK-K8 (RBT 28·05 per cent), there is a narrow peripheral zone of parallel fibred bone in the outer cortex, whereas in the midcortex, fibrolamellar bone with the primary osteons arranged in a laminar pattern is visible (Text-fig. 1C). Although growth rings were absent in the humeri of 90 mm or less in length, a distinct line of arrested growth

TABLE 4. Histological characteristics of the long limb bones of *L. murrayi* examined. Numbers of specimens are given in parentheses. Limb bones are measured in mm.

Skeletal elements	Per cent adult size	Primary bone	Growth rings (LAGs and annuli)	Secondary reconstruction	Other features
1. humeri (12)					
a. HL 25·85 (1)	14·64	WFB, primary channels and globular osteocyte lacunae	none	none	irregular periosteal periphery, MR contains bony trabeculae
b. HL 60–70 (3)	35–40	FLB, laminar arrangement of PO	none	erosionally enlarged channels	–
c. HL 70–100 (6)	40–60		LAGs and annuli in humeri > 90 mm	profuse SO	–
d. HL > 100 (2)	≥ 60	laminar pattern in the deeper cortex; reticular-subplexiform pattern in the outer cortex	cannot be discerned	erosionally enlarged resorption cavities; few SO	–
2. ulnae and radii (3 +3)	50–80	FLB, longitudinally orientated PO	one LAG and annulus in the ulna; two LAGs in the radius (SAM-PK-K8991a)	erosionally enlarged channels in the mid- and outer cortex; profuse SO in deeper cortex	–
3. femora (12)					
a. FL 36·77 (1)	18·75	channels show onset of osteonal deposits – FLB	Two narrow annuli	–	irregular periosteal periphery
b. FL 50–70 mm (5)	25–40	FLB, laminar-subplexiform-reticular arrangement, few radially orientated channels	none	extensive erosionally enlarged resorption cavities and SO	endosteal bone is absent in the femora < 60 mm in length
c. FL 90–120 mm (3)	40–50	FLB, laminar pattern in the inner and mid-cortex, subreticular arrangement in the outer cortex. Abundant radially orientated channels in the outer cortex.	cannot be discerned	extensive erosionally enlarged channels	narrow compact periosteal cortex
d. FL > 120 mm (3)	50–100	FLB, laminar pattern, in places a subreticular-subplexiform arrangement can be seen	one LAG present in the midcortex	erosionally enlarged channels in the inner and mid-cortical region	–
4. Tibia (3) and fibula (1)	55–80	FLB, radially orientated channels	two LAGs in the tibia of SAM-PK-K8991a	erosionally enlarged vascular channels	CCCB in the perimedullary region

(LAG) and an annulus is present in the relatively larger humeri of SAM-PK-K8 (HL 99 mm, Text-fig. 1C) and SAM-PK-K8991a (HL *c.* 100 mm). The cortical thickness (RBT) is more than 30 per cent in humeri greater than 100 mm in length (> *c.* 50 per cent adult size; Table 5). In these humeri, the primary osteons are organized in a laminar pattern in the deeper cortex and are in a reticular-subplexiform pattern in the outer cortex. In ISIR751, the perimedullary region to the midcortex contains erosionally enlarged channels that resulted in a high cortical porosity (about 26 per cent) whereas profuse secondary osteons are visible in the deeper cortical region of SAM-PK-8991a. The medullary region of the humeri contains bony trabeculae of the cancellous bone. Endosteally coated marrow spaces are visible between the bony trabeculae and form sinuses of various diameters.

Ulna and radius. The ulna and radius from three individuals were studied: SAM-PK-11184 (UL 67·5 mm, RL 54·6 mm), SAM-PK-K8991a (UL 78·6 mm, RL 68·02 mm) and SAM-PK-K8013 (UL 118 mm, RL 84 mm). The characteristic features of the ulnae and radii are given in Table 4. The cortical thickness of the ulna is greater than that of the radius measured in the same individual (Table 5). Although growth rings cannot be discerned in the ulna of SAM-PK-11184 because of poor preservation, one prominent LAG and annulus in the inner cortex
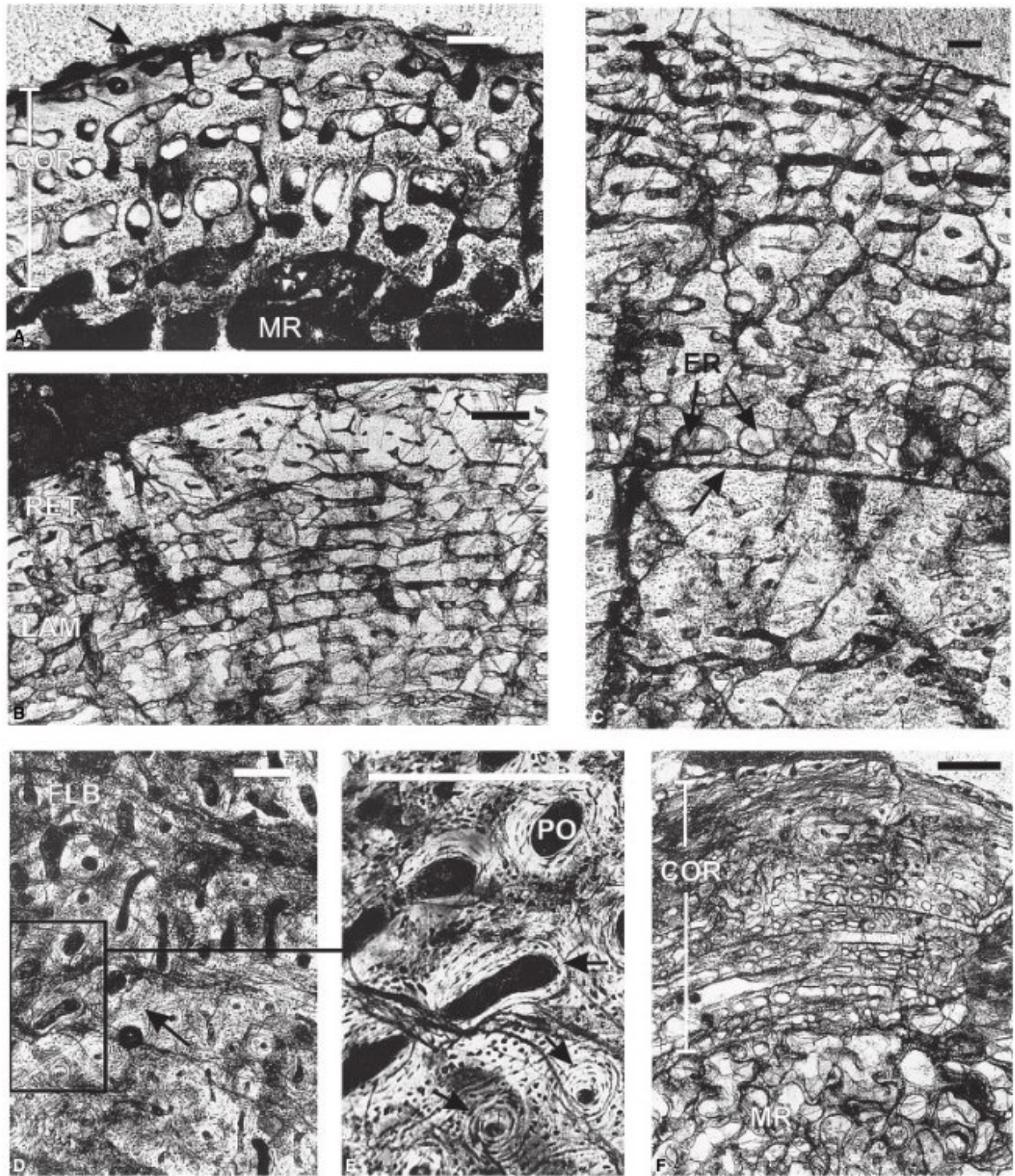
TEXT-FIG. 1. *Lystrosaurus murrayi.* A–C, diaphyseal cross-sections of the humeri. A, SAM-PK-3531, showing the cortex (COR) with longitudinally orientated primary channels. Arrow indicates the uneven peripheral margin. B, SAM-PK-11184, showing the laminar (LAM) and reticular (RET) patterns of the primary osteons in the deeper and outer cortex, respectively. C, SAM-PK-K8, showing a thick cortex with fibrolamellar bone and a prominent LAG (arrow); erosion cavities are marked by ER. D–E, SAM-PK-K8991a, diaphyseal transverse section of the ulna showing D, fibrolamellar bone (FLB) and an LAG (arrow) in the cortex, and E, part of D at higher magnification showing secondary osteons (arrows) in the mid-cortical region. F, SAM-PK-11184, radial transverse section showing erosionally enlarged channels in the cortex (COR) and cancellous bone in the medullary region (MR). Periosteal surface is towards top of the frame. Scale bars represent 200 μm.

TABLE 5. Diaphyseal cortical thickness (RBT) of available limb bones and ribs in the growth series of *L. murrayi*. RBT is expressed as percentage of the total cross-sectional diameter.

Specimen no.	Per cent adult size	Humerus	Radius	Ulna	Femur	Tibia	Rib
SAM-PK-3531	14·64	12·24	–	–	–	–	27·33
ISIR758	18·75	–	–	–	12·76	–	–
ISIR757	35	–	–	–	20·68	–	–
ISIR753	35	17·85	–	–	–	–	–
ISIR751	41·25	23·03	–	–	–	–	–
SAM-PK-K1415	45·86	–	–	–	–	–	28·36
SAM-PK-K8796b	47·26	–	–	–	18·3	–	–
SAM-PK-11184	50·67	22·7	18·46	21·15	22·3	–	–
SAM-PK-K8	56·07	28·05	–	–	–	–	34·26
SAM-PK-K8991a	57·5	31·12	24·07	25·32	–	9·85	–
SAM-PK-K8796a	72·6	–	–	–	25·8	10·33	–
ISIR759	76·51					12·06	
SAM-PK-K8013	76·84	32·5	–	–	–	–	35·17
ISIR752	100	–	–	–	–	–	36·55

(Text-fig. 1D) and another possibly in the outer cortex is seen in SAM-PK-K8991a. Two LAGs are also present in the radial cortex of SAM-PK-K8991a. It also contains erosionally enlarged channels in the mid- and outer cortex, and profuse secondary osteons in the inner cortex (Text-fig. 1E). As in the humerus, the medullary region is completely occupied by cancellous bone in the ulnar and radial diaphyseal sections (Text-fig. 1F).

Femur. Twelve femora of various sizes (FL 36·77–142·43 mm) were examined. ISIR758, the smallest femur (FL 36·77 mm, 18·75 per cent adult size) shows a narrow cortex (RBT 12·76 per cent), a large medullary region and high cortical porosity (23·41 per cent). The cortex is composed of an irregular periosteal periphery, and woven-fibred bone matrix. The channels within the cortex are mostly longitudinally orientated with circumferential and a few radial anastomoses. Most of the vascular channels show centripetal osteonal deposits forming primary osteons and fibrolamellar bone tissue (Text-fig. 2A). Two narrow annuli are present in the outer cortex (Text-fig. 2A).

High porosity (about 12 per cent in ISIR 757) and globular osteocyte lacunae characterize the cortices of the larger femora. The mid-diaphyseal section of ISIR757 (FL 68·66 mm; Text-fig. 2A) shows that the cortical thickness (RBT) is 20·68 per cent, and much thicker than that of ISIR758 (Table 5). Increasingly thicker cortices are evident in longer femora (Table 5). The primary osteons show reticular-subplexiform arrangement in ISIR757 (Text-fig. 2B) whereas laminar and subreticular patterns in the deeper cortex and outer cortex, respectively, are evident in SAM-PK-11184 (Text-fig. 2C). Radially arranged channels are especially abundant in the region of the trochanter major and in the outer cortex. A LAG is present in the mid-cortex of the largest femur (SAM-PK-K8796a: FL 142·43 mm, 72·6 per cent adult size). Endosteal bone deposits are absent in femora less than 60 mm in length. In SAM-PK-11184, several erosion lines are visible showing the deposition of endosteal bone along the edges of the trabeculae (Text-fig. 2D). Erosionally enlarged resorption cavities are present in the inner and mid-cortical region. A few small secondary osteons occur in the outer-midcortex of ISIR757.

Tibia and fibula. A noteworthy feature of the three tibiae (TiL 75·48–88·4 mm) examined is the very narrow cortex in comparison to that of the other elements examined (Table 5). Abundant radially orientated channels are visible in the tibial cortex (Text-fig. 3A, C) of SAM-PK-K8991a and ISIR759. On the other hand, the primary osteons are mainly longitudinally orientated and discrete in SAM-PK-K8796a. Two LAGs are visible in SAM-PK-K8991a. Other features include extensive secondary reconstruction, which resulted in erosionally enlarged vascular channels in the inner and mid-cortex and a narrow compact periosteal cortex. A prominent reversal line separating endosteal and appositional growth, and compacted coarse cancellous bone tissue in the perimedullary region are visible (Text-fig. 3B). Only the metaphyseal region of the fibula (ISIR760: FiL 85·39 mm) was available for study (Text-fig. 3D). The primary osteons are in a subreticular arrangement. Growth rings are absent. There are a few secondary osteons.

Phalanx. The transverse section of a proximal phalanx (SAM-PK-K8796a) shows a narrow cortex (RBT 9·82 per cent). A prominent annulus composed of avascular, lamellar bone is present. Few secondary osteons are visible right at the periosteal margin. The medullary region is completely filled with a dense network of bony trabeculae (Text-fig. 4A). A reversal line separates appositional and endosteal growth.

Vertebra. A transverse section of a dorsal vertebra (SAM-PK-K8012) shows a very narrow cortex. Radially orientated channels are present along the base of the neural canal. Along the periosteal margin in the outer cortex a narrow zone of lamellar bone is present. A distinctive feature of the vertebrae is the presence of a dense network of trabeculae in the medullary region.

Scapula. The scapular blade was studied in two specimens, SAM-PK-K8012 and SAM-PK-K8796a. Its transverse section shows a central cancellous region containing trabeculae, bordered on either side by a narrow compact cortex, and forms a
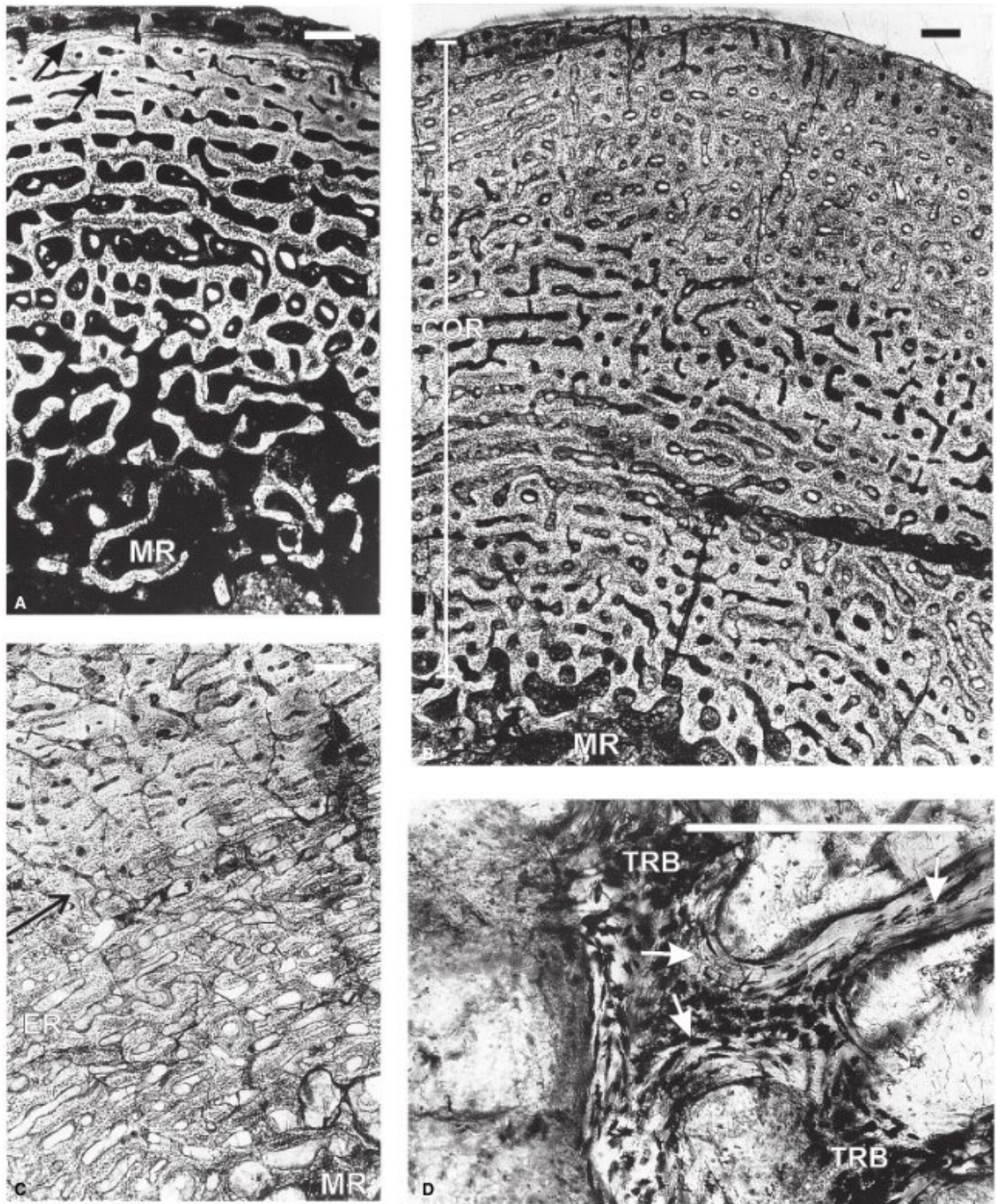
TEXT-FIG. 2. *Lystrosaurus murrayi.* Diaphyseal transverse sections of the femora. A, ISI R758, showing fibrolamellar bone and two narrow undulating annuli in the cortex (arrows). B, ISI R757, showing fibrolamellar bone with reticular-subplexiform arrangement of primary osteons in the cortex (COR). C–D, SAM-PK-11184, showing C, secondarily enlarged erosion cavities in the deeper cortex and a compact outer cortex (an arrow marks the division between the deeper and outer cortex), and D, medullary region with bony trabeculae (TRB) of the cancellous bone and thin deposits of endosteal bone along the edges (arrows). Periosteal surface is towards top of the frame. Scale bars represent 200 µm.
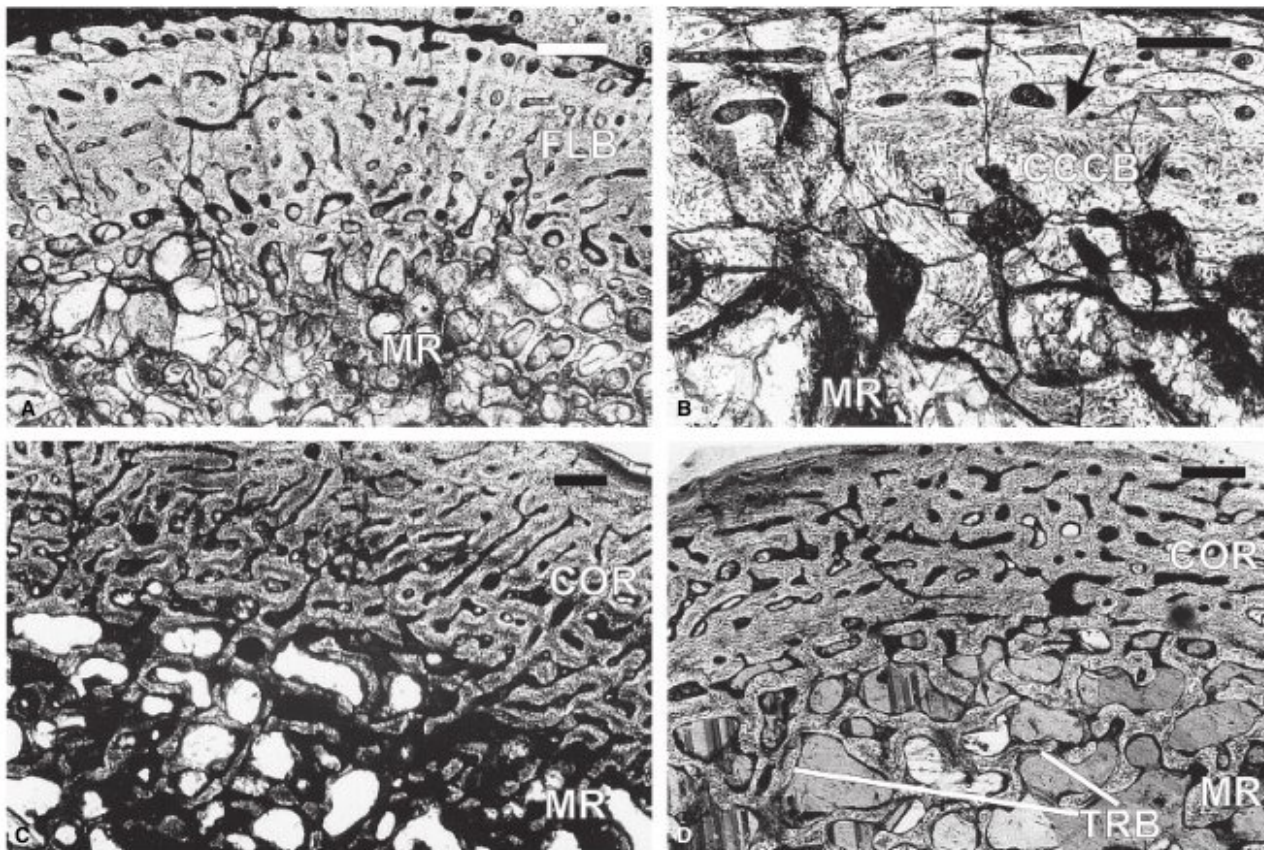
TEXT-FIG. 3. *Lystrosaurus murrayi*. A–C, diaphyseal transverse sections of the tibiae showing A, SAM-PK-K8991a, a narrow cortex with fibrolamellar bone (FLB) and cancellous bone in the medullary region (MR); B, SAM-PK-K8796a, a prominent reversal line (arrow) and a narrow region of compacted coarse cancellous bone (CCCB) in the perimedullary region; C, ISIR 759, radially orientated channels in the cortex (COR). D, ISIR 760, fibula shows trabecular infilling of the medullary region (TRB) and narrow cortical region of compact fibrolamellar bone. Periosteal surface is towards top of the frame. Scale bars represent 200 μm.

diploe (*sensu* Francillon-Vieillot *et al.* 1990). The primary cortical bone is fibrolamellar. The primary osteons are discrete and longitudinally orientated. Growth rings are absent.

Clavicle. Two clavicles, SAM-PK-3531 and ISIR754, were studied. The transverse section of the smaller element, SAM-PK-3531, reveals a thick cortex composed of woven-fibred bone matrix with longitudinally orientated vascular channels, and some containing osteonal deposits (Text-fig. 4B). Growth rings and secondary reconstruction are absent. The transverse section of the larger clavicle (ISIR754) shows a thick cortex (RBT 27·61 per cent) composed of fibrolamellar bone (Text-fig. 4C). In the deeper cortex, a laminar-subplexiform pattern is prevalent whereas in the outer cortex the primary osteons are mostly discrete. Secondarily enlarged vascular canals with wide lumina are seen in the deep and mid-cortical region. Other features include a high porosity, a narrow compact periosteal cortex and absence of growth rings.

Rib. Dorsal ribs (Text-fig. 5) from seven individuals of various sizes (14·64–100 per cent adult size) were examined. The transverse section of the rib of the smallest individual (SAM-PK-3531) shows a thick cortex (RBT 27·33 per cent) composed of

woven-fibred bone matrix. Most of the canals in the deeper cortex are longitudinally orientated with radial and circumferential anastomoses. Some of the channels contain osteonal deposits (Text-fig. 5A). The dorsal rib fragments of larger individuals have increasingly thicker cortex (Table 5). The primary osteons show a laminar-subplexiform arrangement in SAM-PK-11184 whereas in SAM-PK-K8 longitudinally orientated simple channels are present in the cortex. In SAM-PK-K8013 (*c.* 76 per cent adult size), the inner to mid-cortex is composed of fibrolamellar bone tissue whereas a distinct change towards parallel-fibred tissue is observed in the outer cortex (Text-fig. 5B–C). The outer cortex along the periosteal margin is more or less avascular while the primary osteons in the deeper cortex are mainly longitudinally orientated. A distinctive feature of ISIR752 (Text-fig. 5D) is the high prevalence of radially orientated channels. Some of these run from the medullary region to the mid-cortex while others run from the mid-cortex to the periosteal margin. One distinct, but narrow, annulus composed of lamellar bone is present in the midcortex of SAM-PK-K1415. The section of ISIR752 also shows an asymmetric extension of secondary reconstruction towards the medial side, which is probably related to the curvature of the rib (Buffrènil *et al.* 1990).
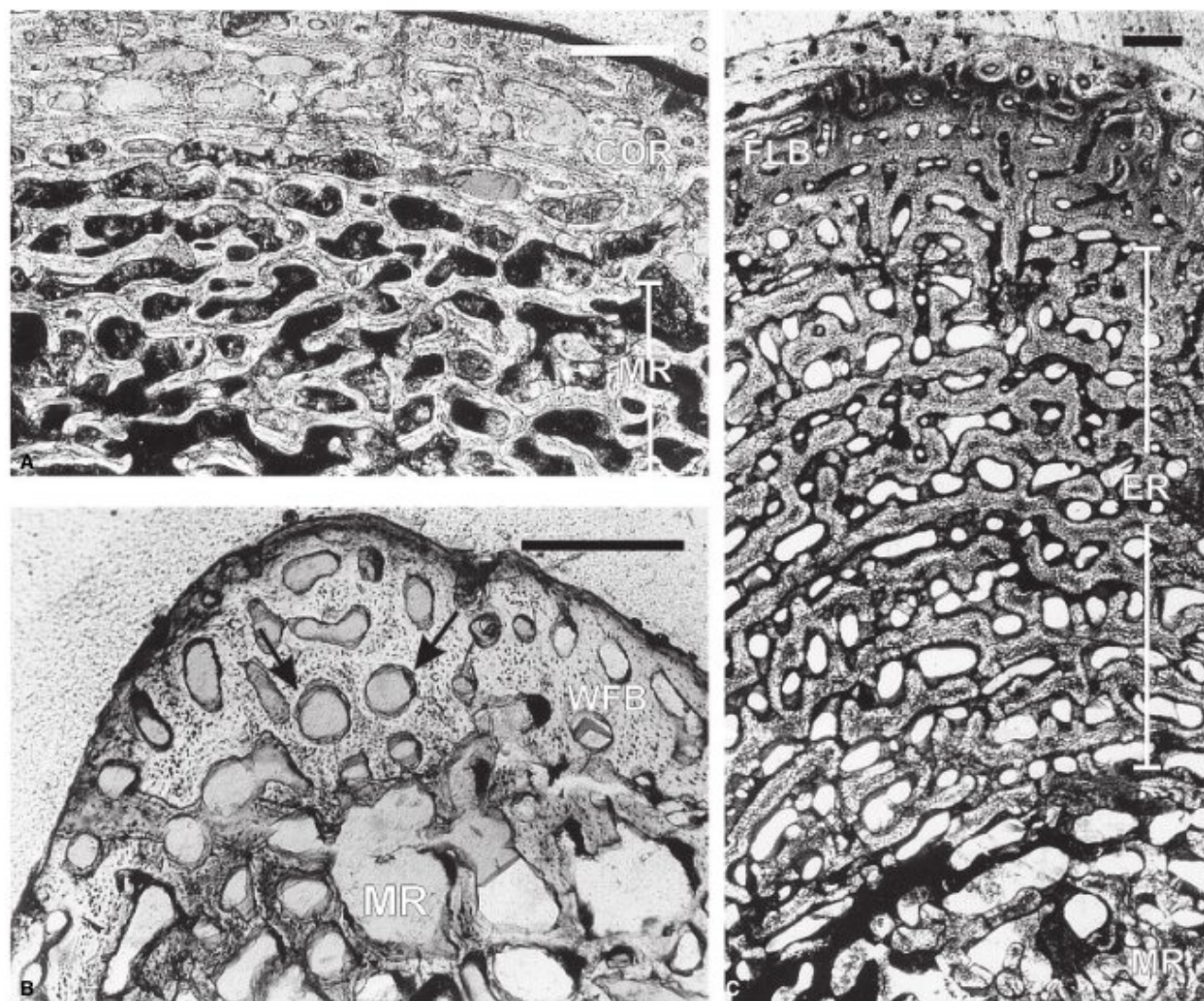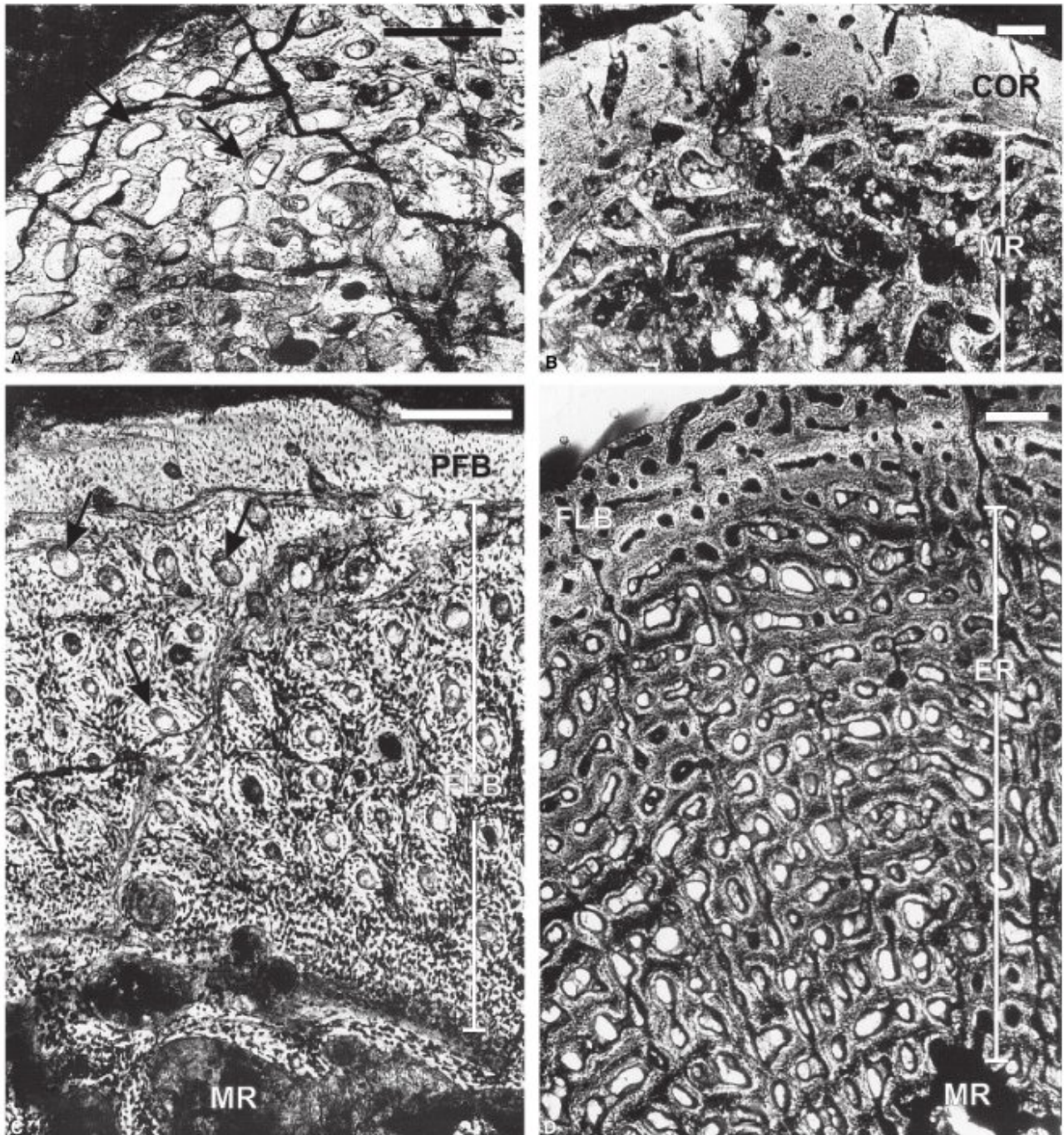
TEXT-FIG. 4. *Lystrosaurus murrayi*. A, SAM-PK-K8796a, transverse section of a proximal phalanx showing a narrow cortex (COR) and a large medullary region filled with bony trabeculae of cancellous bone. B–C, transverse sections of the clavicles showing B, SAM-PK-3531, woven-fibred bone matrix (WFB) and longitudinally orientated bony channels with some osteonal deposits (arrows), and C, ISI R754, extensive secondarily enlarged erosion cavities in the deeper to mid-cortex (ER) and a narrow, relatively compact outer cortex containing fibrolamellar bone (FLB). Periosteal surface is towards top of the frame. Scale bars represent 200 μm.

DISCUSSION

Growth pattern

The bone microstructure of *L. murrayi* shows that the cortex is predominantly composed of woven-fibred bone matrix. Most of the channels within the bone are longitudinally orientated and have circumferential anastomoses. Radially orientated vascular channels are also present in the outer cortex and in the regions of muscle insertion such as the deltopectoral crest, trochanter major and base of the neural canal, depending on the skeletal element. The channels show centripetal osteonal deposits forming primary osteons, and, together with the woven-fibred bone matrix, results in fibrolamellar bone (Text-figs 1–5). Similar occurrences of fibrolamellar bone with primary osteons in a laminar-plexiform pattern in lystrosaurid limb bones were observed by Ricqlès (1972). Our study has shown that in specimens such as SAM-PK-K8991a and SAM-PK-11184 (i.e. HL > 90 mm) the primary osteons are mainly arranged in a laminar-sub-plexiform pattern in the inner to mid-cortex whereas the outer cortical region shows a reticular pattern (Text-fig. 2D). Fibrolamellar bone is considered to indicate rapid osteogenesis (Amprino 1947; Buffrénil 1980; Reid 1990; Chinsamy 1997; Margerie *et al.* 2002) and suggests overall fast growth of *L. murrayi*. The predominance of fibrolamellar bone in the various skeletal

TEXT-FIG. 5. *Lystrosaurus murrayi.* Transverse sections of the dorsal ribs. A, SAM-PK-3531, showing bony channels with some osteonal deposits (arrows). B–C, SAM-PK-K8013 showing B, nearly avascular compact cortex (COR) and a large medullary region (MR) with cancellous bone, and C, a thick cortex with peripheral avascular parallel-fibred bone (PFB), and fibrolamellar bone (FLB) and profuse secondary osteons (arrows) in the deeper cortex. D, ISIR752, showing fibrolamellar bone (FLB) and extensive secondarily enlarged erosion cavities in the cortex (ER). Periosteal surface is towards top of the frame. Scale bars represent 200 μm.

elements of *L. murrayi* is in contrast to that seen in many extant nonavian sauropsids, except some crocodilians and juvenile chelonians (Reid 1984, 1996; Chinsamy 1995). However, this tissue type has been identified in many other extinct vertebrates such as the dinosaurs, captorhinids, pterosaurs, pelycosaurs, gorgonopsians and cynodonts (Gross 1934; Enlow and Brown 1957; Enlow 1969; Ricqlès 1969, 1976, 1983; Chinsamy 1990, 1995;

Ricqlès *et al.* 1991; Curry 1999; Horner *et al.* 1999, 2000; Botha and Chinsamy 2000).

Four distinct ontogenetic regimes, evident within the inferred overall fast growth strategy of *L. murrayi*, are summarized in Table 6. The woven-fibred bone matrix of the cortex, initiation of fibrolamellar bone, high local porosity and absence of LAGs characterized the first or early juvenile stage (Text-fig. 6A), and are best exemplified by the smallest individual SAM-PK-3531 (HL < 30 mm; 14·64 per cent adult size). During this stage, *L. murrayi* had rapid growth without any interruptions. Endosteal bone deposition and secondary reconstruction were absent in this stage. The rapid growth of the first stage suggested by the highly vascularized fibrolamellar bone (Text-fig. 6B) continued in the second phase of growth (late juvenile stage; HL 30–60 mm, FL *c.* 35–65 mm). An annulus suggesting temporary slowed growth is present only in the femur (ISIR758, FL 36·77 mm), which may indicate adverse local environmental conditions. A note-

TABLE 6. Characteristic bone microstructure in the four growth stages of *L. murrayi.*

Early juvenile (< 15 per cent adult size)
  Appositional deposition of woven-fibred bone matrix
  Longitudinally and radially orientated channels in the cortices
  Highly uneven and irregular periosteal margin
  No LAGs
  No secondary reconstruction
  No endosteal bone deposition
Late juvenile (*c.* 15–30 per cent adult size)
  Fibrolamellar bone tissue in the cortex
  Primary osteons arranged in laminar-subplexiform pattern
  No LAGs
  Secondary reconstruction; erosionally enlarged vascular channels, very few secondary osteons
  Medullary cavity contains cancellous bone
Sub-adult (*c.* 30–60 per cent adult size)
  Primary fibrolamellar bone tissue in the cortex
  LAGS and annuli present
  Absence of a free medullary cavity; filled with trabeculae
  Extensive secondary reconstruction; resorption cavities even in the outer cortex
  Onset of endosteal bone deposition
Adult (> 60 per cent adult size)
  Cortex generally composed of fibrolamellar bone tissue
  Primary osteons arranged in laminar pattern in the inner cortex while mid-to outer cortex shows subreticular organization and radially orientated channels
  Ribs show narrow avascular peripheral zones of parallel-fibred bone tissue
  Annuli and LAGs present
  Extensive secondary reconstruction relative to other stages; profuse secondary osteons in the deeper cortex
  Compacted coarse cancellous bone and dense network of bony trabeculae in the medullary region

worthy feature in the late juvenile stage was the presence of secondary reconstruction, which resulted in erosionally enlarged vascular channels in the inner cortical region. Other features in this stage included the presence of cancellous bone in the medullary region, and the absence of endosteal bone deposition (Text-fig. 6B).
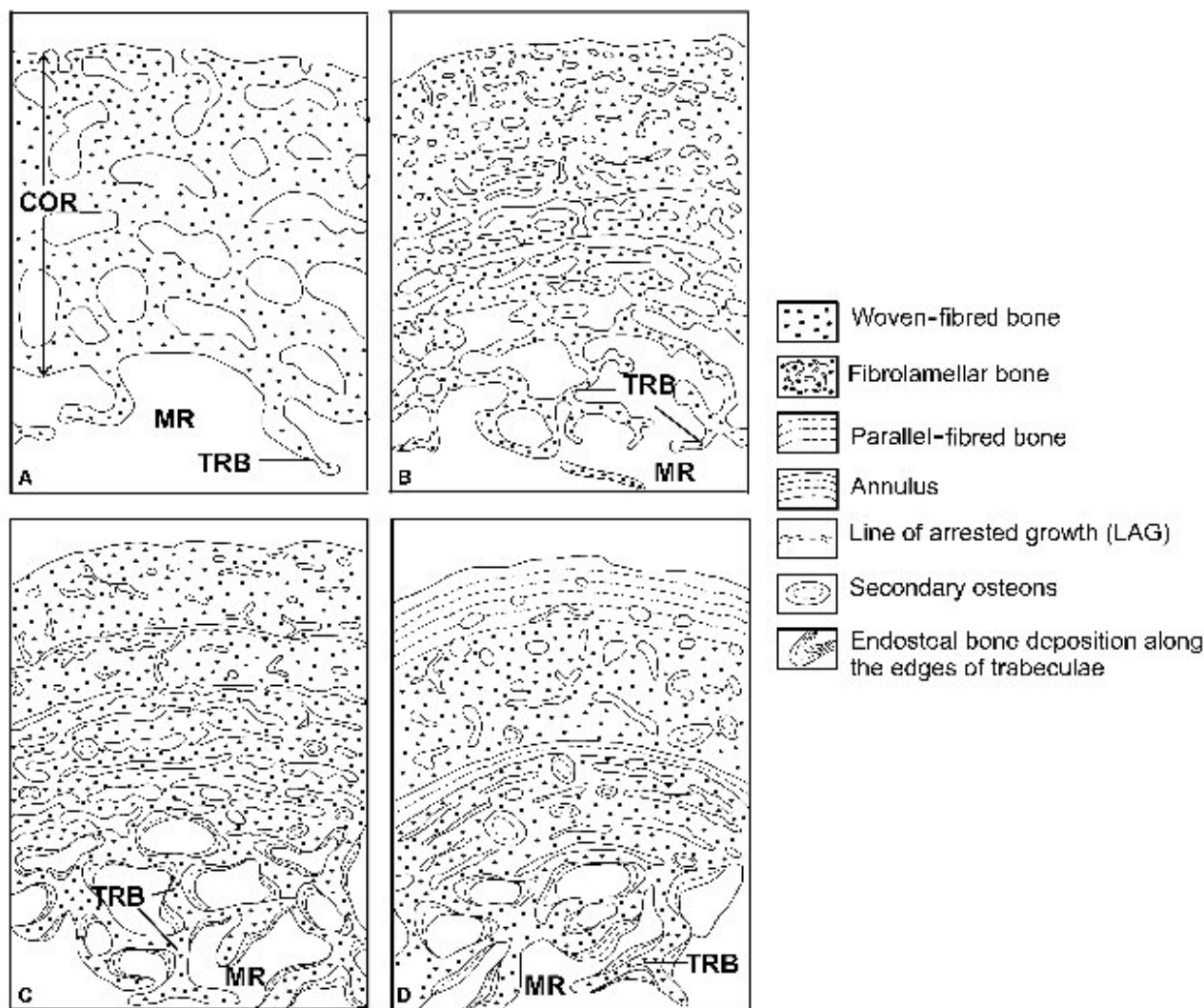
Subsequent appearance of LAGs (Text-fig. 6C) in larger individuals, such as SAM-PK-K8 and SAM-PK-K8991a, suggests periodic cessation of growth in the third growth stage C (i.e. sub-adult stage; HL 60–100 mm, FL *c.* 65–120 mm). The annuli and LAGs were followed by resumption of rapid growth, as shown by wide zones of fibrolamellar bone (Chinsamy and Rubidge 1993; Horner *et al.* 2000). LAGs and annuli have been associated with environmental stress, as suggested by their occurrence in extant crocodilians (Hutton 1986), some rodents (Klevezal 1996) and Arctic polar bears (Chinsamy *et al.* 1998). In general, the Triassic climate was dry and hot with seasonal rainfall (Hiller and Stavrakis 1984; Wing and Sues 1992). It is probable that annuli and/or LAGs developed in *L. murrayi* during these dry and adverse conditions when growth slowed or stopped completely. Starck and Chinsamy (2002) concluded that the LAGs are an expression of a high degree of developmental plasticity (*sensu* Smith-Gill 1983) suggesting the ability of the animal to stop growth and development during unfavourable conditions. It is a functional trait that allows an individual to adjust to changing external conditions. Presence of such LAGs in several individuals suggests that *L. murrayi* had developmental flexibility and could stop growing in hostile environments. The sub-adult stage also marked the onset of endosteal bone deposition along the edges of the trabeculae in the medullary region (Text-fig. 6C).

A general decrease in periosteal osteogenesis and slow growth rate later in ontogeny (i.e. in adults; HL > 100 mm, FL > 120 mm) is inferred from the more organized patterns of the primary osteons, the appearance of growth rings and the change in the peripheral tissue type from woven-fibred to parallel-fibred (Text-fig. 6D). The latter is especially evident in the microstructure of the dorsal ribs (SAM-PK-K8013; Text-fig. 5C–D), where the peripheral bone is nearly avascular, and parallel-fibred, and the osteocyte lacunae show linear orientation. A narrow zone of lamellar bone is also present in the outer cortex of the vertebra (SAM-PK-K8012). Such parallel-fibred and lamellar bone in skeletal elements implies very slow growth during this stage. However, growth did not stop completely, as suggested by absence of external circumferential lamellae and thick deposition of parallel-fibred bone, thereby indicating an indeterminate growth strategy for *Lystrosaurus*.

In summary, the bone microstructure suggests that the growth strategy of *L. murrayi* involved distinct ontogenetic variation, and this variation can be correlated with

TEXT-FIG. 6. Schematic representation of bone microstructure in the four ontogenetic stages of *L. murrayi*. A, early juvenile; B, late juvenile; C, sub-adult; and D, adult stages. Periosteal surface is towards the top of the page.

size classes of *L. murrayi* as deduced from allometric/ regression equations, skeletal morphology and relative size of the specimens. The juveniles (including early and late stages comprising individuals with HL < 60 mm, FL < 65 mm and < 30 per cent adult size) had fast, sustained growth, which became interrupted in the sub-adult stage (HL 60–100 mm, FL *c.* 65–120 mm, 30–60 per cent adult size). In the adult stage (HL > 100 mm, FL > 120 mm, >60 per cent adult size), growth slowed down appreciably.

Histovariation

A distinctive feature of the bone microstructure of *L. murrayi* is the inter-elemental histovariability, especially

evident where several elements of the same individual were examined (Table 1). These variations relate to the thickness of the cortex (RBT), organization of the primary osteons, which may be observed locally within the same section, incidence of annuli and LAGs, and extent of secondary reconstruction. The cortical thickness of the humerus is much higher than that of the other limb bones (Table 5, Text-fig. 7) even within the same individual (e.g. SAM-PK-K8991a), suggesting a higher rate of appositional growth relative to the other limb bones. Similar fast growth of the humerus relative to other limb bones was noted in the small dicynodont *Diictodon* (Ray and Chinsamy 2004) and in the extant Japanese quails (Starck and Chinsamy 2002). An interesting feature seen in *L. murrayi* is the high cortical thickness of the ribs compared to the limb bones even in the early juvenile

TEXT-FIG. 7. Different skeletal elements showing variable trends in the cortical/relative bone wall thickness (RBT) with increase in size. Juveniles: < 30 per cent adult size; sub-adults: 30–60 per cent adult size; adults: > 60 per cent adult size.
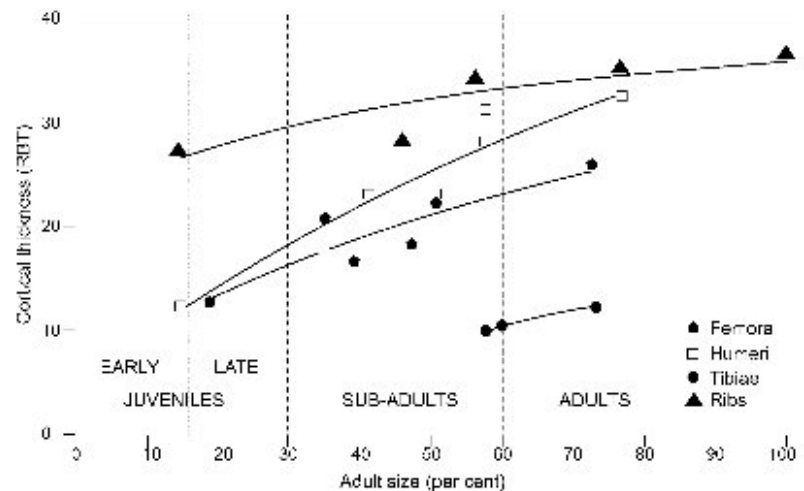
stage and within the same individual (Text-fig. 7): RBT in SAM-PK-3531 is 27·33 per cent while that of the humerus is only 12·24 per cent (Table 5). A variable arrangement of the primary osteons is seen in most of the skeletal elements studied, where the observed pattern often ranges from laminar to subplexiform and reticular. Such variable organization was also seen in *Diictodon* (Ray and Chinsamy 2004) and in some other non-mammalian therapsids (Ricqlès 1972; Ray *et al*. 2004). Similar inter-elemental histovariation was observed in the dinosaurs *Apatosaurus* (Curry 1999) and *Maiasaura* (Horner *et al*. 2000). As bone histology is affected by a variety of factors such as phylogenetic, ontogenetic, functional and biomechanical constraints (Ricqlès 1972; Ricqlès *et al*. 1991; Reid 1996; Curry 1999; Starck and Chinsamy 2002) such variation is expected and suggests variable growth rate of the skeletal elements.

Lifestyle adaptations

Wall (1983) considered the thickness of the cortex (RBT) to be correlated with a specific mode of life. He suggested that if the cortex exceeds 30 per cent of the average bone diameter in most of the limb bones, then the animal was at least semi-aquatic (e.g. hippo, manatee, beaver). The high RBT of aquatic/semi-aquatic animals suggests high bone density, which helps in overcoming buoyancy. High bone densities have also been recorded in the sirenians, cetaceans and certain aquatic birds (Buffrénil *et al*. 1990; Hua and Buffrénil 1996). Similar high values of cortical thickness are seen in *Crocodylus niloticus* (36·3 per cent; Chinsamy 1991) and *Alligator* (36·45 per cent; Ray and Chinsamy 2004), which corroborate Wall's findings. However, such a high value of RBT is also seen in *Diictodon*, inferred to be a digging dicynodont, where the hum-

eral and femoral cortical thickness is about 34 per cent in adult individuals (Ray and Chinsamy 2004), and contrasts with Wall's findings.

In *L. murrayi*, only the humeral cortical thickness exceeds 30 per cent of the bone diameter (e.g. 32·5 per cent in SAM-PK-K8013, *c*. 76 per cent adult size), and is much higher than that of other limb bones examined, suggesting enhanced weight of the forelimb. In addition, the rate of increase in humeral RBT from 12·24 to 32·5 per cent (14·64–76·84 per cent adult size) is much higher than that of other limb bones (Text-fig. 7) and cannot be explained by increase in size through ontogeny alone. It suggests a different functional constraint for the forelimb, which was probably used actively for digging and/or swimming, especially by the adult individuals.

However, the most distinctive feature of *L. murrayi* is the high cortical thickness of its dorsal ribs relative to the other bones throughout growth (Table 5, Text-fig. 7). This is evident even in the juvenile individual (SAM-PK-3531) where the RBT of the rib is much higher than that of its humerus (Text-fig. 7). In SAM-PK-8013 (76·84 per cent adult size), the cortical thickness of the rib is 35·17 per cent (Table 5). However, this high cortical thickness of the dorsal ribs contrasts with that of the inferred burrowing dicynodont, *Diictodon* (SAM-PK-K6704, RBT *c*. 20 per cent). The thick and highly vascularized cortices of the ribs along with nearly complete filling of the medullary region by cancellous bone (Text-fig. 5) probably suggest pachyostosis of the ribs (*sensu* Ricqlès and Buffrénil 2001) of *L. murrayi* similar to that seen in the semi-aquatic *Claudiosaurus* (Buffrénil and Mazin 1989), where no extensive external morphological modification is visible. The thick ribs of *Lystrosaurus* in comparison to that of other dicynodonts were also noted by Retallack *et al*. (2003).

Previous work has shown that distinct histological specializations are indicative of different modes of life

(Nopsca 1930; Ricqlès 1974, 1977; Rhodin 1985; Buffrénil and Schoevart 1988; Buffrénil and and Mazin 1990; Hua and Buffrénil 1996; Sheldon 1997; Damiani 2000; Ricqlès and Buffrénil 2001; Steyer *et al.* in press). In aquatic animals, these specializations involve either reduction or increase in skeletal mass (Chinsamy 1997). The bone microstructure of *L. murrayi* at different stages of growth is characterized by an extensive development of cancellous bone in the medullary region of a variety of skeletal elements including the diaphyseal regions of the limb bones (Text-figs 1–5). In the sub-adult and adult stages, the bone trabeculae contained thin deposits of lamellar endosteal bone forming successive layers separated from each other by erosion lines. This suggests that the trabeculae have undergone several localized erosion–reconstruction cycles (Buffrénil and Schoevart 1988; Horner *et al.* 2001). Such infilling by the trabeculae of coarse cancellous bone resulted in the near absence of a 'tubular structure' of the limb bones (*sensu* Ricqlès and Buffrénil 2001).

This absence of a free medullary region occurs in conjunction with extensive secondary reconstruction, which constitutes about 70–90 per cent of the total cortical area in the adult stage. The secondary remodelling starts early in ontogeny (in the late juvenile stage) and most of the channels within the bone are erosionally enlarged, resulting in high local bone porosity (e.g. about 23 per cent in ISIR758) and an almost cancellous appearance. In the sub-adult and adult stages, the compact part of the cortex is limited to a narrow layer in the peripheral region. Profuse secondary osteons are especially visible in the adult radius and ulna (e.g. SAM-PK-K8991a).

The trabeculae in the medullary region augment density (Carter and Spengler 1978), flexural rigidity, strength and toughness of the bones (Rogers and Laberbera 1993) whereas extensive secondary reconstruction, a time-dependent process, includes resorption of bone channels and subsequent centripetal deposition of lamellated bone inside the enlarged cavities resulting in the formation of secondary osteons (Ricqlès *et al.* 1991). In *L. murrayi*, secondary reconstruction started early in ontogeny (in the late juvenile stage) and resulted in erosionally enlarged vascular channels, an apparent increase in cortical porosity, narrow compact cortex and profuse secondary osteons in the deeper cortex. Although a medullary spongiosa is common in the dicynodonts (Chinsamy and Rubidge 1993), such an association with extensive secondary reconstruction that occupied 70–90 per cent of the cortex has not yet been recorded in any other dicynodonts. The genera examined include *Endothiodon*, *Wadiasaurus* (pers. obs.), *Cistecephalus*, *Oudenodon*, *Dicynodon*, other dicynodontids and *Kannemeyeria* (Ricqlès 1972; Chinsamy and Rubidge 1993), and even *Diictodon* (Chinsamy and Rubidge 1993; Ray and Chinsamy 2004), which has been inferred to be a digging dicynodont (Ray and Chinsamy 2003). In these dicynodonts, the secondary reconstructions were mainly found to be restricted to the perimedullary region. Even in neotherapsids such as the gorgonopsians *Scylacops* and *Aelurognathus*, the therocephalian *Pristerognathus*, the cynodonts *Procynosuchus*, *Tritylodon* (Ray *et al.* 2004), *Diademodon* and *Cynognathus* (Botha and Chinsamy 2000), such an association between medullary spongiosa and extensive secondary reconstruction was not noted. Such bone microstructure is usually found in tetrapods secondarily adapted to an aquatic/semi-aquatic lifestyle (Buffrénil and Mazin 1990; Ricqlès *et al.* 1991; Damiani 2000; Ricqlès and Buffrénil 2001). Medullary spongiosa results in increasing tissue compactness in the medullary and deep cortical region (Buffrénil and Mazin 1989), and in turn suggests at least a semi-aquatic lifestyle for *L. murrayi*.

However, *L. murrayi* exhibits differing modification of the limb bones for a semi-aquatic lifestyle. This is revealed in the extent and nature of secondary reconstruction, which varies depending on loading and position of the skeletal element (Lieberman and Pearson 2001), even within the same individual, and in the extent of cortical compactness. Secondary reconstruction is generally higher in the midshafts of distal limb bones, especially in the radius and ulna, relative to that of the proximal limb bones, which results in profuse secondary osteons and shows an overall increase in compactness and mass in ontogeny. A similar increase in mass is also evident in the ribs and vertebrae. In contrast, skeletal elements such as the humerus, femur and clavicle show very little or no centripetally deposited secondary bone within the resorption cavities, even in the adult stage. This suggests an imbalance between destructive (osteoclastic) and reconstructive (osteoblastic) stages (Enlow 1963) that resulted in an apparent increase in cortical porosity and an osteoporotic-like state in the adult humerus, femur and clavicle, and a tendency towards a reduction in mass. Thus, histological specializations of *L. murrayi* relating to its inferred adaptation to a semi-aquatic life do not follow either one of the two opposite patterns (that is, increase or decrease in skeletal mass) seen in many other aquatic and semi-aquatic animals such as claudiosaurs, ichthyosaurs and turtles. Instead, as suggested by Ricqlès and Buffrénil (2001) for extant manatees, the osteohistological features in *Lystrosaurus* are variously combined and not mutually exclusive.

CONCLUSIONS

The bone microstructure of *L. murrayi* reveals that the cortex is predominantly composed of fibrolamellar bone. Most of the primary osteons are longitudinally orientated and have circumferential anastomoses resulting in laminar-sub-plexiform-reticular patterns. Predominance of fibrolamellar bone suggests rapid osteogenesis and fast overall growth of

L. murrayi. Within this overall fast growth strategy, four distinct ontogenetic stages may be inferred from the bone microstructure. During the early juvenile stage (HL < 30 mm), the bone microstructure is characterized by woven-fibred bone matrix, initiation of fibrolamellar bone, absence of growth rings and high cortical porosity that suggest sustained fast growth. In the late juvenile stage (HL 30–60 mm, < 30 per cent adult size) fast growth continued. The subsequent appearance of LAGs suggests periodic cessation of growth in the sub-adult stage (HL 60–100 mm, 30–60 per cent adult size). This stage also marked the onset of endosteal bone deposition. Growth slowed down appreciably in the last/adult stage (HL > 100 mm, > 60 per cent adult size) as evident from the more organized patterns of the primary osteons and the change in peripheral tissue type from fibrolamellar to parallel-fibred bone.

The absence of external circumferential lamellae and continued deposition of parallel-fibred bone suggest an indeterminate growth strategy for *Lystrosaurus.* Interelemental histovariability is evident, especially where several skeletal elements from the same individual were examined. These variations relate to the thickness of the cortex, organization of the primary osteons, incidence of annuli and LAGs, and extent of secondary reconstruction.

L. murrayi is characterized by the high cortical thickness of its dorsal ribs (*c.* 35 per cent), even in the juvenile stage (*c.* 27 per cent), which possibly suggests pachyostosis of the ribs though no gross external morphological modifications are visible.

The bone microstructure, from the late juvenile stage onwards, is characterized by a medullary spongiosa and extensive secondary reconstruction that resulted in a narrow compact cortex. This feature is in contrast to that found in other dicynodonts examined, and is more similar to that of semi-aquatic/aquatic animals. At least a semi-aquatic lifestyle for *L. murrayi* is proposed here.

REFERENCES

AMPRINO, R. 1947. La structure du tissu osseux envisagée comme l'expression de différences dans la vitesse de l'accroissement. *Archives de Biologie,* **58**, 315–330.

BOTHA, J. and CHINSAMY, A. 2000. Growth patterns deduced from the histology of the cynodonts *Diademodon* and *Cynognathus. Journal of Vertebrate Paleontology,* **20**, 705–711.

BROOM, R. 1932. *The mammal-like reptiles of South Africa and the origin of mammals.* H. F. & G. Witherby, London, 376 pp.

BUFFRÉNIL, V. DE 1980. Mise en evidence de l'incidence des conditions de milieu sur la croissance de *Crocodylus siamensis* (Schneider 1801) et valeur des marques de croissance squelettiques pour l'evaluation de l'age individual. *Archives de Zoologie Experimentale Generale,* **121**, 63–76.

—— and MAZIN, J. M. 1989. Bone histology of *Claudiosaurus germaini* (Reptilia, Claudiosauridae) and the problem of pachyostosis in aquatic tetrapods. *Historical Biology,* **2**, 311–322.

—— —— 1990. Bone histology of the ichthyosaurs: comparative data and functional interpretation. *Paleobiology,* **16**, 435–447.

—— and SCHOEVART, D. 1988. On how the periosteal bone of the delphinid humerus becomes cancellous: ontogeny of a histological specialization. *Journal of Morphology,* **198**, 149–164.

—— RICQLÉS, A. DE, RAY, C. E. and DOMNING, D. P. 1990. Bone histology of the ribs of the *Archaeocetes* (Mammalia: Cetacea). *Journal of Vertebrate Paleontology,* **10**, 455–466.

BÜHLER, P. 1986. Das Vogelskelett-hochentwickelter knochenleichtbau. *Arcus,* **5**, 221–228.

CARTER, D. R. and SPENGLER, D. M. 1978. Mechanical properties and composition of cortical bone. *Clinical Orthopaedics and Related Research,* **135**, 192–217.

CHINSAMY, A. 1990. Physiologic implications of the bone histology of *Syntarsus rhodesiensis* (Saurischia: Theropoda). *Palaeontologia Africana,* **27**, 77–82.

—— 1991. The osteohistology of femoral growth within a clade: a comparison of the crocodile, *Crocodylus niloticus,* the dinosaurs, *Massospondylus* and *Syntarsus* and the birds, *Struthio* and *Sagittarius.* Unpublished PhD thesis, University of the Witwatersrand, Johannesburg, 200 pp.

—— 1993*a*. Bone histology and growth trajectory of the prosauropod dinosaur *Massospondylus carinatus* Owen. *Modern Geology,* **18**, 319–329.

—— 1993*b*. Image analysis and the physiological implications of the vascularization of femora in archosaurs. *Modern Geology,* **19**, 101–108.

—— 1995. Ontogenetic changes in the bone histology of the Late Jurassic ornithopod *Dryosaurus lettowvorbecki. Journal of Vertebrate Paleontology,* **15**, 96–104.

—— 1997. Assessing the biology of the fossil vertebrates through bone histology. *Palaeontologia Africana,* **33**, 29–35.

—— and DODSON, P. 1995. Inside a dinosaur bone. *American Scientist,* **83**, 174–180.

—— and RAATH, M. A. 1992. Preparation of fossil bone for histological examination. *Palaeontologia Africana,* **29**, 39–44.

—— and RUBIDGE, B. S. 1993. Dicynodont (Therapsida) bone histology: phylogenetic and physiological implications. *Palaeontologia Africana,* **30**, 97–102.

—— RICH, T. and VICKERS-RICH, P. 1998. Polar dinosaur bone histology. *Journal of Vertebrate Paleontology,* **18**, 385–390.

CLUVER, M. A. 1971. Cranial morphology of the dicynodont genus *Lystrosaurus*. *Annals of the South African Museum*, **56**, 155–274.

COLBERT, E. H. 1974. *Lystrosaurus* from Antarctica. *American Museum Novitates*, **2535**, 1–44.

COPE, E. D. 1870. Remarks by Edward D. Cope at a meeting May 6th 1870. *Proceedings of the American Philosophical Society*, **11**, 419.

COSGRIFF, J. W., HAMMER, W. R. and RYAN, W. J. 1982. The Pangaean reptile *Lystrosaurus maccaigi* in the Lower Triassics of Antarctica. *Journal of Palaeontology*, **56**, 371–385.

CURRY, K. A. 1999. Ontogenetic histology of *Apatosaurus* (Dinosauria: Sauropoda): new insights on growth rates and longevity. *Journal of Vertebrate Paleontology*, **19**, 654–665.

DAMIANI, R. J. 2000. Bone histology of some Australian Triassic temnospondyl amphibians: preliminary data. *Modern Geology*, **24**, 109–124.

ENLOW, D. H. 1963. *Principles of bone remodeling*. Charles C. Thomas, Springfield, 123 pp.

—— 1969. The bones of reptiles. 45–80. *In* GANS, C. (ed.). *Biology of the Reptilia 1*. Academic Press, New York, 373 pp.

—— and BROWN, S. O. 1957. A comparative histological study of fossil and recent bone tissue 2. *Texas Journal of Science*, **9**, 186–214.

FRANCILLON-VIEILLOT, H., BUFFRÉNIL, V. DE, CASTANET, J., GERANDIE, J., MEUNIER, F. J., SIRE, J. Y., ZYLBERBERG, L. L. and RICQLÈS, A. DE 1990. Microstructure and mineralization of vertebrate skeletal tissues. 471–530. *In* CARTER, J. G. (ed.). *Skeletal biomineralization: patterns, process and evolutionary trends 1*. Van Nostrand Reinhold, New York, 832 pp.

GROENWALD, G. H. 1991. Burrow casts from the *Lystrosaurus-Procolophon* Assemblage Zone, Karoo sequence, South Africa. *Koedoe*, **34**, 13–22.

GROSS, W. 1934. Die Typen des mikroskopischen Knochenbaues bei foslen Stegocephalen und Reptilien. *Zeitschrift fur Anatomie*, **103**, 731–764.

HILLER, N. and STAVRAKIS, N. 1984. Permo-Triassic systems in the southeastern Karoo Basin, South Africa. *Palaeogeography, Palaeoclimatology, Palaeoecology*, **45**, 1–21.

HORNER, J. R., PADIAN, K. and RICQLÈS, A. DE 2001. Comparatve osteohistology of some embryonic and perinatal archosaurs: developmental and behavioral implications for dinosaurs. *Paleobiology*, **27**, 39–58.

—— RICQLÈS, A. and PADIAN, K. 1999. Variation in dinosaur skeletochronology indicators: implications for age assessment and physiology. *Paleobiology*, **25**, 295–304.

—— —— —— 2000. Long bone histology of the hadrosaurid dinosaur *Maiasaura peeblesorum*: growth dynamics and physiology based on an ontogenetic series of skeletal elements. *Journal of Vertebrate Paleontology*, **20**, 115–129.

HUA, S. and BUFFRÉNIL, V. DE 1996. Bone histology as a clue for the interpretation of the functional adaptations in the Thalattosuchia (Reptilia, Crocodylia). *Journal of Vertebrate Paleontology*, **16**, 703–717.

HUTTON, J. M. 1986. Age determination of living Nile crocodiles from the cortical stratification of bone. *Copeia*, **1986**, 332–341.

HUXLEY, T. H. 1859. On a new species of *Dicynodon* (*D. murrayi*) from near Colesberg, South Africa, and on the structure of the skull in the dicynodonts. *Quarterly Journal of the Geological Society of London*, **15**, 649–658.

KING, G. M. 1991. The aquatic *Lystrosaurus*: a paleontological myth. *Historical Biology*, **4**, 285–321.

—— and CLUVER, M. A. 1991. The aquatic *Lystrosaurus*: an alternative lifestyle. *Historical Biology*, **4**, 323–341.

—— and JENKINS, I. 1997. The dicynodont *Lystrosaurus* from the Upper Permian of Zambia: evolutionary and stratigraphical implications. *Palaeontology*, **40**, 149–156.

KLEVEZAL, G. A. 1996. *Recording structures of mammals*. A. A. Balkema, Brookfield, 274 pp.

LIEBERMAN, D. E. and PEARSON, O. M. 2001. Trade-off between modeling and remodeling responses to loading in the mammalian limb. *Bulletin of the Museum of Comparative Zoology*, **156**, 269–282.

MARGERIE, E. DE, CUBO, J. and CASTANET, J. 2002. Bone typology and growth rate: testing and quantifying 'Amprino's rule' in the mallard (*Anas platyrhynchos*). *Comptes Rendus de l'Académie des Sciences, Série Biologiques*, **325**, 221–230.

NOPSCA, F. 1930. Notes on Stegocephalia and Amphibia. *Proceedings of the Zoological Society of London*, **64**, 979–995.

OWEN, R. 1860. On some reptilian fossils from South Africa. *Quarterly Journal of the Geological Society of London*, **16**, 49–54.

PETERS, R. H. 1989. *The ecological implication of body size*. Cambridge University Press, Cambridge, 329 pp.

RAY, S. and CHINSAMY, A. 2003. Functional aspects of the postcranial anatomy of the Permian dicynodont *Diictodon* and its ecological implications. *Palaeontology*, **46**, 151–183.

—— —— 2004. *Diictodon feliceps* (Therapsida, Dicynodontia): bone histology, growth and biomechanics. *Journal of Vertebrate Paleontology*, **24**, 180–194.

—— BOTHA, J. and CHINSAMY, A. 2004. Bone histology and growth patterns of some nonmammlian therapsids. *Journal of Vertebrate Paleontology*, **24**, 634–648.

REID, R. E. H. 1984. Primary bone and dinosaurian physiology. *Geological Magazine*, **121**, 589–598.

—— 1990. Zonal 'growth rings' in dinosaurs. *Modern Geology*, **15**, 19–48.

—— 1996. Bone histology of the Cleveland-Lloyd dinosaurs and of dinosaurs in general, Part I: Introduction: introduction to bone tissues. *Geology Studies*, **41**, 25–71.

RETALLACK, G. J., SMITH, R. M. H., and WARD, P. D. 2003. Vertebrate extinction across P–T boundary in Karoo Basin, South Africa. *Geological Society of America, Bulletin*, **115**, 1133–1152.

RHODIN, A. G. J. 1985. Comparative chondro-osseous development and growth of marine turtles. *Copeia*, **1985**, 752–771.

RICQLÈS, A. DE 1969. Recherches paléohistologiques sur les os longs des Tétrapodes. II, Quelques observations sur la structure des longs des Thériodontes. *Annales de Paléontologie (Vertébrés)*, **55**, 1–52.

—— 1972. Recherches paléohistologiques sur les os longs des Tétrapodes. III, Titanosuchiens, Dinocéphales et Dicynodontes. *Annales de Paléontologie (Vertébrés)*, **58**, 17–60.

—— 1974. Evolution of endothermy: histological evidence. *Evolutionary Theory*, **1**, 51–80.

—— 1976. On bone histology of fossil and living reptiles with comments on its functional and evolutionary significance. 123–149. *In* BELLAIRS, A. d'A and COX, C. B. (eds). *Morphology and biology of reptiles*. Linnean Society Symposium Series, **3**. Academic Press, London, 290 pp.

—— 1977. Recherches paléohistologiques sur le os longes des tétrapodes. VII. – Sur la classification, la signification fonctionnelle et l'histoire des tissues osseus des tétrapodes. *Annales de Paléontologie (Vertébrés)*, **63**, 33–56.

—— 1983. Cyclical growth in the long limb bones of a sauropod dinosaur. *Acta Palaeontologia Polonica*, **28**, 225–232.

—— and BUFFRÉNIL, V. DE 2001. Bone histology, heterochronies and the return of tetrapods to life in water: where are we? 289–310. *In* MAZIN, J. M. and BUFFRÉNIL, V. DE (eds). *Secondary adaptation of tetrapods to life in water*. Verlag Dr. Friedrich Pfeil, Munchen, Germany, 367 pp.

—— MEUNIER, F. J., CASTANET, J. and FRANCILON-VIEILLOT, H. 1991. Comparative microstructure of bone. 1–77. *In* HALL, B. K. (ed.). *Bone 3: bone matrix and bone specific products*. CRC Press Inc., Boca Raton, 282 pp.

ROGERS, R. R. and LABERBERA, M. 1993. Contribution of internal bony trabeculae to the mechanical properties of the humerus of the pigeons (*Columba livia*). *Journal of Zoology*, **230**, 433–441.

SANDER, P. M. 2000. Long bone histology of the Tendaguru sauropods: implications for growth and biology. *Paleobiology*, **26**, 466–488.

SEEBACHER, F. 2001. A new method to calculate allometric length-mass relationships of dinosaurs. *Journal of Vertebrate Paleontology*, **21**, 51–60.

SHELDON, M. A. 1997. Ecological implications of mosasaur bone microstructure. 333–354. *In* CALLAWAY, J. M. and NICHOLLS, E. L. (eds). *Ancient marine reptiles*. Academic Press, New York, 501 pp.

SMITH, R. M. H. and WARD, P. D. 2001. Patterns of vertebrate extinctions across an event bed at the Permo-Triassic boundary in the Karoo Basin of South Africa. *Geology*, **29**, 1147–1150.

SMITH-GILL, S. J. 1983. Developmental plasticity: developmental conversion versus phenotypic modulation. *American Zoologist*, **23**, 47–55.

STARCK, J. M. and CHINSAMY, A. 2002. Bone microstructure and developmental plasticity in birds and other dinosaurs. *Journal of Morphology*, **254**, 232–246.

STEYER, J. S., LAURIN, M., CASTANET, J. and RICQLÈS, A. DE in press. First histological and skeletochronological data on temnospondyl growth, palaeoecological and palaeoclimatological implications. *Palaeogeography, Palaeoclimatology, Palaeoecology*.

TRIPATHI, C. and SATSANGI, P. P. 1963. *Lystrosaurus* fauna of the Panchet series of the Raniganj coalfield. *Palaeontologia Indica, Memoirs of Geological Survey of India*, **37**, 1–55.

WALL, W. P. 1983. The correlation between high limb bone density and aquatic habits in recent mammals. *Journal of Palaeontology*, **57**, 197–207.

WATSON, D. M. S. 1912. The skeleton of *Lystrosaurus*. *Records of the Albany Museum*, **2**, 287–299.

—— 1913. The limbs of *Lystrosaurus*. *Geological Magazine*, **10**, 256–258.

WING, S. L. and SUES, H. D. 1992. Mesozoic and early Cenozoic ecosystems. 327–416. *In* BEHRENSMEYER, A. K., DAMUTH, J. D., DIMICHELE, W. A., POTTS, R., SUES, H. D. and WING, S. L. (eds). *Terrestrial ecosystems through time*. University of Chicago Press, Chicago, 568 pp.

APPENDIX

Abbreviations used in the text-figures, plates and tables

CCCB, compacted coarse cancellous bone; COR, cortex; ER, erosionally enlarged channels; FiDD, diameter of the distal fibula; FiL, length of the fibula; FL, femoral length; FLB, fibrolamellar bone tissue; FMD, diameter of femoral midshaft; FPD, diameter of proximal femur; HL, humeral length; HMD, diameter of humeral midshaft; HPD, diameter of proximal humerus; LAG, line of arrested growth; LAM, laminar arrangement of the primary osteons (*sensu* Ricqles *et al.* 1991); MR, medullary region; n, number of specimens measured; PFB, parallel-fibred bone; PO, primary osteons; RET, reticular arrangement of the primary osteons (*sensu* Ricqles *et al.* 1991); RL, radial length; RMD, diameter of the radial midshaft; RPD, diameter of the proximal radius; SO, secondary osteons; TiDD, diameter of the distal tibia; TiL, tibial length; TRB, trabeculae; UL, length of ulna; UPD, diameter of the proximal ulna; WFB, woven-fibred bone; x, length; y, different dimensions.